

available at www.sciencedirect.comjournal homepage: www.elsevier.com/locate/ijrefrig

Effect of CuO nanolubricant on R134a pool boiling heat transfer

M.A. Kedzierski^{a,*}, M. Gong^b

^aNational Institute of Standards and Technology, Bldg. 226, Rm B114, Gaithersburg, MD 20899, USA

^bChinese Academy of Sciences, Beijing, China

ARTICLE INFO

Article history:

Received 25 February 2008

Received in revised form 17

December 2008

Accepted 19 December 2008

Published online ■

Keywords:

Heat exchanger

Pool boiling

Experiment

Heat transfer

Binary mixture

Polyolester

R134a

Additive

Particle

Copper oxide

ABSTRACT

This paper quantifies the influence of CuO nanoparticles on the boiling performance of R134a/polyolester mixtures on a roughened, horizontal, flat surface. A lubricant based nanofluid (nanolubricant) was made with a synthetic ester and CuO particles. For the 0.5% nanolubricant mass fraction, the nanoparticles caused a heat transfer enhancement relative to the heat transfer of pure R134a/polyolester (99.5/0.5) of between 50% and 275%. A smaller enhancement was observed for the R134a/nanolubricant (99/1) mixture, which had a heat flux that was on average 19% larger than that of the R134a/polyolester (99/1) mixture. Further increase in the nanolubricant mass fraction to 2% resulted in a still smaller boiling heat transfer improvement of approximately 12% on average. Thermal conductivity measurements and a refrigerant/lubricant mixture pool-boiling model were used to suggest that increased thermal conductivity is responsible for only a small portion of the heat transfer enhancement due to nanoparticles.

© 2008 Elsevier Ltd and IIR. All rights reserved.

Effet de l'oxyde de cuivre utilisé comme nanolubrifiant sur l'échange de chaleur lors de l'ébullition libre du R134a

Mots clés : échangeur de chaleur ; ébullition libre ; expérimentation ; transfert de chaleur ; mélange binaire ; polyolester ; R134a ; additif ; particule ; oxyde de cuivre

* Corresponding author. Tel.: +1 301 975 5282; fax: +1 301 975 8973.

E-mail address: mark.kedzierski@nist.gov (M.A. Kedzierski).

0140-7007/\$ – see front matter © 2008 Elsevier Ltd and IIR. All rights reserved.

doi:10.1016/j.ijrefrig.2008.12.007

Nomenclature*English symbols*

A_n	regression constant in Table 1 $n = 0, 1, 2, 3$
k	thermal conductivity, $\text{W K}^{-1} \text{m}^{-1}$
L_y	length of test surface (Fig. 2), m
q''	average wall heat flux, W m^{-2}
T	temperature, K
T_w	temperature at roughened surface, K
U	expanded uncertainty
u_i	standard uncertainty

Greek symbols

ΔT_s	wall superheat: $T_w - T_s$, K
ϕ	volume fraction

English subscripts

CuO	R134a/RL68H1Cu mixture
L	nanolubricant
p	pure R134a
PL	R134a/RL68H mixture
q''	heat flux
s	saturated state
T_w	wall temperature,
w	wall, heat transfer surface

1. Introduction

Government research initiatives have supported an explosion of research in recent years including the investigation of the heat transfer properties of liquids with dispersed nano-size particles called nanofluids. Prior to these initiatives, nanofluids research was mainly confined to thermal conductivity investigations. Eastman et al. (2001) found that the thermal conductivity of some nanofluids, with nanoparticles at a volume fraction of less than 0.4%, was more than 40% greater than that of the pure base fluid. Herein lies what is believed to be a great potential for the enhancement of liquid heat transfer by the addition of nanoparticles to the base fluid.

Water, ethylene glycol, and lubricants have been successfully used as base fluids in making stable nanofluids where the particles remain suspended in the liquid. Although water based nanofluids are the least stable of the three liquids because of the relatively low viscosity of water, most of the boiling heat transfer studies have been conducted with water based nanofluids (Bang and Chang, 2004; Wen and Ding, 2005; You et al., 2003). Of these previous studies, You et al. (2003) and Bang and Chang (2004) did not observe a pool-boiling enhancement with nanofluids; however, Wen and Ding (2005) did. Consequently, boiling heat transfer improvements can be obtained with nanofluids even though the mechanisms that govern the improvement are not fully understood.

Currently, there are no published measurements to determine if nanoparticles can be used to improve refrigerant/lubricant boiling heat transfer. Bi et al. (2007) examine the effect of nanoparticles on the performance of a refrigerator, thus, giving an indirect account of the effect of nanoparticles on refrigerant/lubricant flow boiling. One reason for the lack of pool-boiling heat transfer investigations might be the expectation that once the nanolubricant is mixed with the refrigerant, the nanoparticles will become unstable with respect to the refrigerant/lubricant mixture because the relatively low viscosity of the mixture discourages Brownian motion. This potential outcome, however, may not prohibit the application of nanoparticles to air-conditioning equipment because the mechanism of the boiling heat transfer of refrigerant/lubricant mixtures is strongly governed by the lubricant excess layer that resides at the boiling surface (Kedzierski, 2003a). Similar to the way a lubricant excess layer is established, the boiling will drive the nanoparticles to the

heat transfer surface where they will become stable and remain within the viscous lubricant excess layer. Some of the particles will also be entrained in the vigorous boiling of the fluid. If the nanoparticles significantly change the thermal conductivity of the lubricant excess layer, that may cause an enhancement or a degradation in heat transfer depending on whether the increased conduction causes a reduced available superheat or whether it increases the thermal boundary layer thickness. The potential for a boiling heat transfer enhancement is likely to depend on the material of the particles, their shape, size, distribution, and concentration.

In order to investigate the influence of nanoparticles on refrigerant/lubricant pool boiling, the boiling heat transfer of three R134a/nanolubricant mixtures on a roughened, horizontal, flat (plain), copper surface was measured. A commercial polyolester lubricant (RL68H¹), commonly used with R134a chillers, with a nominal kinematic viscosity of $72.3 \mu\text{m}^2/\text{s}$ at 313.15 K was the base lubricant that was mixed with nominally 30 nm diameter copper (II) oxide (CuO) nanoparticles. Copper (II) oxide (79.55 g/mol) has many commercial applications including use as an optical glass-polishing agent. A manufacturer used a proprietary surfactant at a mass between 5% and 15% of the mass of the CuO as a dispersant for the RL68H/CuO mixture (nanolubricant). The manufacturer made the mixture such that 9% of the volume was CuO particles. The mixture was diluted in-house to a 1% volume fraction of CuO by adding neat RL68H (Kedzierski and Gong, 2007) and ultrasonically mixing the solution for approximately 24 h. The particle size and dispersion were verified by a light scattering technique several weeks after mixing. The particles were approximately 35 nm and well dispersed with little particle agglomeration (Sung, 2006). The RL68H/CuO (99/1)² volume fraction mixture, a.k.a. RL68H1Cu, was mixed with pure R134a to obtain three R134a/RL68H1Cu mixtures at nominally 0.5%, 1%, and 2% nanolubricant mass.

¹ Certain commercial equipment, instruments, or materials are identified in this paper in order to specify the experimental procedure adequately. Such identification is not intended to imply recommendation or endorsement by the National Institute of Standards and Technology, nor is it intended to imply that the materials or equipment identified are necessarily the best available for the purpose.

² The equivalent mixture is RL68H/CuO (94.4/5.6) in terms of mass.

In addition, the boiling heat transfer of three R134a/RL68H mixtures (0.5%, 1%, and 2% mass fractions), without nanoparticles, was measured to serve as a baseline for comparison to the RL68H1Cu mixtures.

2. Apparatus

Fig. 1 shows a schematic of the apparatus that was used to measure the pool-boiling data of this study. More specifically, the apparatus was used to measure the liquid saturation temperature (T_s), the average pool-boiling heat flux (q''), and the wall temperature (T_w) of the test surface. The three principal components of the apparatus were the test chamber, the condenser, and the purger. The internal dimensions of the test chamber were 25.4 mm × 257 mm × 1.54 m. The test chamber was charged with approximately 7 kg of refrigerant, giving a liquid height of approximately 80 mm above the test surface. As shown in Fig. 1, the test section was visible through two opposing, flat 150 mm × 200 mm quartz windows. The bottom of the test surface was heated with high velocity (2.5 m/s) water flow. The vapor produced by liquid boiling on the test surface was condensed by the brine-cooled, shell-and-tube condenser and returned as liquid to the pool by gravity. Further details of the test apparatus can be found in Kedzierski (2002, 2001a).

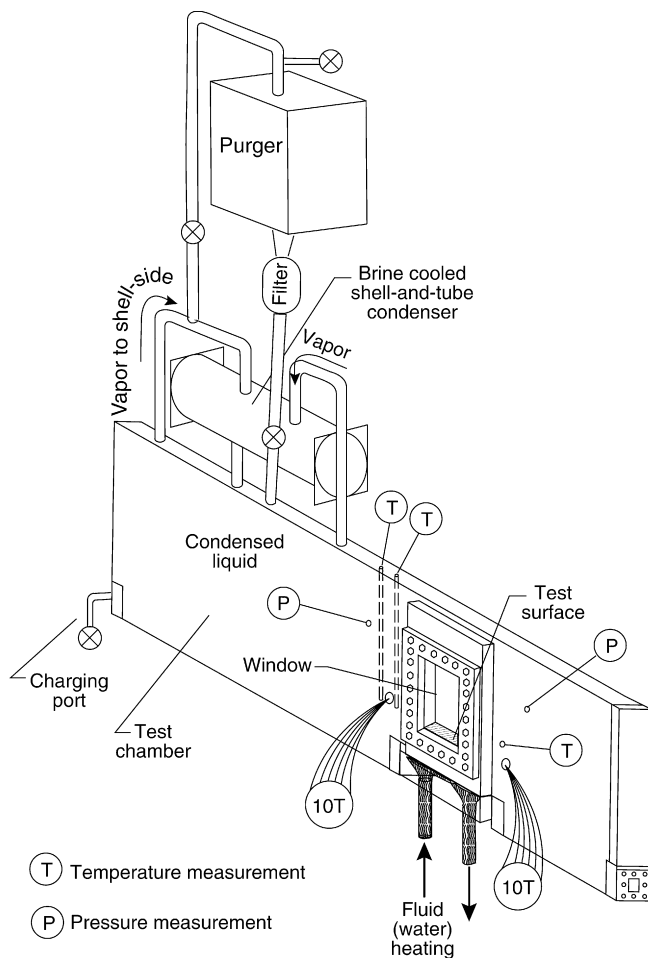


Fig. 1 – Schematic of test apparatus.

3. Test surface

Fig. 2 shows the oxygen-free high-conductivity (OFHC) copper flat test plate that was used in this study. The test plate was machined out of a single piece of OFHC copper by electric discharge machining (EDM). A tub grinder was used to finish the heat transfer surface of the test plate with a crosshatch pattern. Average roughness measurements were used to estimate the range of average cavity radii for the surface to be between 12 μm and 35 μm. The relative standard uncertainty of the cavity measurements were approximately ±12%. Further information on the surface characterization can be found in Kedzierski (2001a).

4. Measurements and uncertainties

The standard uncertainty (u_i) is the positive square root of the estimated variance u_i^2 . The individual standard uncertainties are combined to obtain the expanded uncertainty (U), which is calculated from the law of propagation of uncertainty with a coverage factor. All measurement uncertainties are reported at the 95% confidence level except where specified otherwise. For the sake of brevity, only an outline of the basic measurements and uncertainties is given below. Complete detail on the heat transfer measurement techniques and uncertainties can be found in Kedzierski (2000) and Kedzierski and Gong (2007), respectively.

All of the copper-constantan thermocouples and the data acquisition system were calibrated against a glass-rod standard platinum resistance thermometer (SPRT) and a reference voltage to a residual standard deviation of 0.005 K. Considering the fluctuations in the saturation temperature during the test and the standard uncertainties in the calibration, the expanded uncertainty of the average saturation temperature was no greater than 0.04 K. Consequently, it is believed that the expanded uncertainty of the temperature measurements was less than 0.1 K.

Twenty 0.5 mm diameter thermocouples were force fitted into the wells of the side of the test plate shown in Fig. 2. The

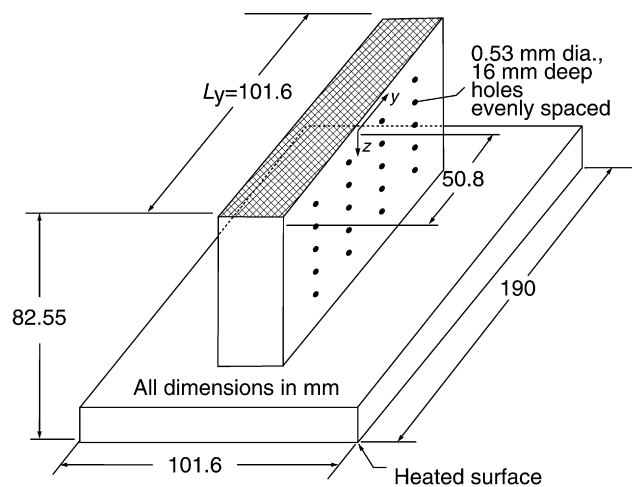


Fig. 2 – OFHC copper flat test plate with cross-hatched surface and thermocouple coordinate system.

heat flux and the wall temperature were obtained by regressing the measured temperature distribution of the block to the governing two-dimensional conduction equation (Laplace equation). In other words, rather than using the boundary conditions to solve for the interior temperatures, the interior temperatures were used to solve for the boundary conditions following a backward stepwise procedure given in Kedzierski (1995).³ Fourier's law and the fitted constants from the Laplace equation were used to calculate the average heat flux (q'') normal to and evaluated at the heat transfer surface based on its projected area. The average wall temperature (T_w) was calculated by integrating the local wall temperature (T). The wall superheat was calculated from T_w and the measured temperature of the saturated liquid (T_s). Considering this, the relative expanded uncertainty in the heat flux ($U_{q''}$) was greatest at the lowest heat fluxes, approaching 10% of the measurement near 10 kW/m². In general, the $U_{q''}$ remained approximately within 3% and 6% for heat fluxes greater than 30 kW/m². The average random error in the wall superheat (U_{T_w}) was between 0.04 K and 0.1 K. Plots of $U_{q''}$ and U_{T_w} versus heat flux can be found in Kedzierski and Gong (2007).

5. Experimental results

The boiling heat flux was varied approximately between 10 kW/m² and 120 kW/m² to simulate a range of possible operating conditions for R134a chillers. All pool-boiling tests were taken at 277.6 K saturated conditions. The data were recorded consecutively starting at the largest heat flux and descending in intervals of approximately 4 kW/m². The descending heat flux procedure minimized the possibility of any hysteresis effects on the data, which would have made the data sensitive to the initial operating conditions (Memory and Marto, 1992). The measured heat flux and wall superheat for all the data of this study and the number of test days and data points for each fluid are tabulated in Kedzierski and Gong (2007). The first few days (1–4) of testing were excluded from the repeatable data sets that are reported here. The “breaking-in” of a surface used to boil refrigerant/lubricant and/or refrigerant/additive mixtures is a common characteristic and typically becomes longer for increasing lubricant or additive mass fraction (Kedzierski, 2006).

The mixtures were prepared by charging the test chamber (see Fig. 1) with pure R134a to a known mass. Next, a measured mass of well-mixed nanolubricant or lubricant was injected with a syringe through a port in the test chamber. The refrigerant/lubricant solution was mixed by flushing pure refrigerant through the same port where the lubricant was injected. All compositions were determined from the masses of the charged components and are given on a mass fraction basis. The maximum uncertainty of the composition measurement is approximately 0.02%, e.g., the range of a 2.0% composition is between 1.98% and 2.02%. Nominal or target mass compositions are used in the discussion. For example, the “actual”

³ For the record, Kedzierski and Gong (2007) provide functional forms of the Laplace equation that were used in this study in the same way as was done in Kedzierski (1995) and in similar studies by this author.

mass composition of the RL68H in the R134a/RL68H (99.5/0.5) mixture was $0.53\% \pm 0.02\%$. Likewise, the RL68H mass fractions for R134a/RL68H (99/1) and the R134a/RL68H (98/2) mixtures were $1.04\% \pm 0.02\%$ and $2.10\% \pm 0.02\%$, respectively. Using the same uncertainties, the nanolubricant mass fractions as tested with R134a were 0.53%, 1.05%, and 1.99%.

The test apparatus was cleaned between the R134a/lubricant and R134a/nanolubricant tests by introducing clean R134a and a sacrificial boiler that was used to remove the lubricant from the test chamber and test surface. The test surface was lightly scrubbed with acetone and a copper cleaner. This procedure was repeated until the pure R134a boiling performance was reproduced.

Fig. 3 is a plot of the measured heat flux (q'') versus the measured wall superheat ($T_w - T_s$) for pure R134a at a saturation temperature of 277.6 K. The closed circles represent 13 days of boiling measurements made over a period of approximately three weeks. The solid lines shown in Fig. 3 are cubic best-fit regressions or estimated means of the data. Five of the 145 measurements were removed before fitting because they were identified as “outliers” based on having both high influence and high-leverage (Belsley et al., 1980). Table 1 gives the constants for the cubic regression of the superheat versus the heat flux for all of the fluids tested here. The residual standard deviation of the regressions – representing the proximity of the data to the mean – vary between 0.07 K and 0.45 K (Kedzierski and Gong, 2007). The dashed lines to either side of the mean represent the lower and upper 95% simultaneous (multiple-use) confidence intervals for the mean. Table 2 shows the average magnitude of 95% multi-use confidence interval for mean for each test fluid. From the confidence intervals, the expanded uncertainty of the estimated mean wall superheat was 0.14 K and 0.06 K for superheats less than and greater than 7 K, respectively.

The effect of the pure lubricant mass fraction on R134a/lubricant pool boiling is shown in Fig. 4. Fig. 4 plots the measured heat flux (q'') versus the measured wall superheat ($T_w - T_s$) at a saturation temperature of 277.6 K for the three R134a/RL68H mixtures. Comparison of the three mean boiling curves shows that the superheats are within approximately 1 K of each other for heat fluxes between approximately 30 kW/m² and 90 kW/m². For the same heat flux range, the

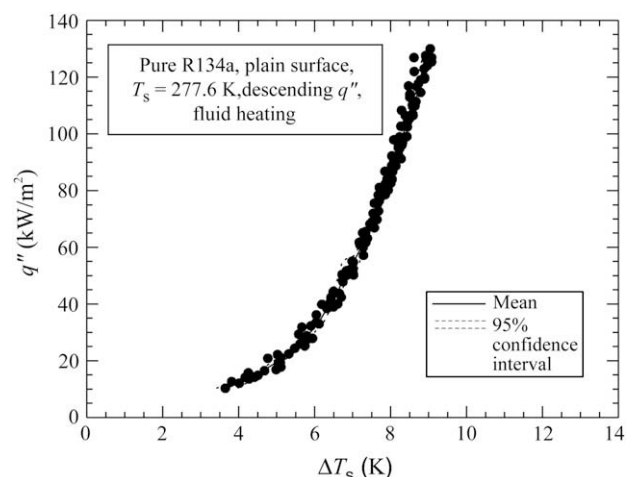


Fig. 3 – Pure R134a boiling curve for plain surface.

Table 1 – Estimated parameters for cubic boiling curve fits for plain copper surface $\Delta T_s = A_0 + A_1 q'' + A_2 q''^2 + A_3 q''^3$ ΔT_s in K and q'' in W/m^2

Fluid	A_0	A_1	A_2	A_3
Pure R134a				
3 K $\leq \Delta T_s \leq 7$ K	1.41341	2.70461×10^{-4}	-5.22703×10^{-9}	3.94517×10^{-14}
7 K $\leq \Delta T_s \leq 9$ K	3.99702	7.78356×10^{-5}	-4.89337×10^{-10}	1.44222×10^{-15}
R134a/RL68H (99.5/0.5)				
4.3 K $\leq \Delta T_s \leq 9.5$ K	1.66769	3.15055×10^{-4}	-4.19310×10^{-9}	1.77327×10^{-14}
9.5 K $\leq \Delta T_s \leq 10.2$ K	1.04922	2.64699×10^{-4}	-2.48124×10^{-9}	7.59925×10^{-15}
R134a/RL68H (99/1)				
4.6 K $\leq \Delta T_s \leq 9.7$ K	1.00155	4.33942×10^{-4}	-7.83196×10^{-9}	5.15712×10^{-14}
9.7 K $\leq \Delta T_s \leq 11.3$ K	9.14630	-3.72774×10^{-5}	1.28138×10^{-9}	-6.85804×10^{-15}
R134a/RL68H (98/2)				
4 K $\leq \Delta T_s \leq 8.5$ K	-5.53159	1.77713×10^{-3}	-7.97232×10^{-8}	1.23223×10^{-12}
8.5 K $\leq \Delta T_s \leq 10.5$ K	7.09007	5.83429×10^{-5}	-2.74470×10^{-10}	1.13436×10^{-16}
R134a/RL68H1Cu (99.5/0.5)				
3.4 K $\leq \Delta T_s \leq 8.2$ K	7.52004×10^{-1}	3.15645×10^{-4}	-4.69784×10^{-9}	2.20673×10^{-14}
R134a/RL68H1Cu (99/1)				
3.5 K $\leq \Delta T_s \leq 9$ K	6.0058×10^{-1}	3.28260×10^{-4}	-1.31501×10^{-9}	-4.42454×10^{-14}
9 K $\leq \Delta T_s \leq 10.7$ K	4.51615	1.84658×10^{-4}	-2.18782×10^{-9}	9.58136×10^{-15}
R134a/RL68H1Cu (99/2)				
3.5 K $\leq \Delta T_s \leq 8.75$ K	3.00385×10^{-2}	6.44828×10^{-4}	-1.79772×10^{-8}	1.78650×10^{-13}
8.75 K $\leq \Delta T_s \leq 12$ K	7.65055	-2.18447×10^{-5}	1.37521×10^{-9}	-7.45213×10^{-15}

superheat for the pure R134a is roughly 3 K less than that for the mixtures translating into a heat transfer degradation with respect to R134a. Kedzierski (2001b) has shown that, in general, degradations due to increased lubricant mass fractions occur when the concentration induced bubble size reduction, and its accompanying loss of vapor generation per bubble, is not compensated by an increase in site density. Once a heat transfer degradation has occurred, it has been observed to continue to degrade with respect to increasing lubricant mass fraction (Kedzierski, 2001b). All the measurements shown in Fig. 4 excluding those for the (98/2) mixture where the heat flux is greater than 30 kW/m² are consistent with this trend. Consequently, the observation that the heat transfer degradation increases from the (99.5/0.5) mixture to the (99/1) mixture and then decreases from the (99/1) mixture to the (98/2) mixture, for heat fluxes greater than 30 kW/m², is unusual and unexpected. In addition, Fig. 4 and Table 2 illustrate a second unusual characteristic of the measurements in that they become more repeatable for the larger lubricant concentrations. More specifically, the average magnitude of the 95% multi-use confidence interval for the mean superheat decreases from 0.22 K, to 0.15 K, and to 0.09 K for increasing mixture compositions of (99.5/0.5), (99/1), and (98/2), respectively. This trend is contrary to what is typically observed for increasing lubricant mass fraction refrigerant/lubricant mixture boiling heat transfer measurements, which usually exhibit increasing data scatter.

The effect of the nanolubricant mass fraction on R134a/nanolubricant pool boiling is shown in Fig. 5. Fig. 5 is a plot of the measured heat flux (q'') versus the measured wall superheat ($T_w - T_s$) for the R134a/RL68H1Cu mixtures at a saturation temperature of 277.6 K. An average of 153 measurements were made for each mixture over the span of approximately a week. The means of the R134a/RL68H1Cu (99/1) and the R134a/

RL68H1Cu (98/2) superheat measurements are within approximately 1 K for the entire heat flux range that was tested. For heat fluxes less than approximately 30 kW/m² and greater than approximately 60 kW/m², the R134a/RL68H1Cu (99/1) mixture mean superheat is less than that of the R134a/RL68H1Cu (98/2) mixture. For heat fluxes between these limits, the R134a/RL68H1Cu (98/2) mixture exhibits the unusual

Table 2 – Average magnitude of 95% multi-use confidence interval for mean $T_w - T_s$ (K)

Fluid	u (K)
Pure R134a	
3 K $\leq \Delta T_s \leq 7$ K	0.14
7 K $\leq \Delta T_s \leq 9$ K	0.06
R134a/RL68H (99.5/0.5)	
4.3 K $\leq \Delta T_s \leq 9.5$ K	0.22
9.5 K $\leq \Delta T_s \leq 10.2$ K	0.22
R134a/RL68H (99/1)	
4.6 K $\leq \Delta T_s \leq 9.7$ K	0.15
9.7 K $\leq \Delta T_s \leq 11.3$ K	0.14
R134a/RL68H (98/2)	
4 K $\leq \Delta T_s \leq 8.5$ K	0.09
8.5 K $\leq \Delta T_s \leq 10.5$ K	0.04
R134a/RL68H1Cu (99.5/0.5)	
3.4 K $\leq \Delta T_s \leq 8.2$ K	0.26
R134a/RL68H1Cu (99/1)	
3.5 K $\leq \Delta T_s \leq 9$ K	0.18
9 K $\leq \Delta T_s \leq 10.7$ K	0.34
R134a/RL68H1Cu (99/2)	
3.5 K $\leq \Delta T_s \leq 8.75$ K	0.15
8.75 K $\leq \Delta T_s \leq 12$ K	0.24

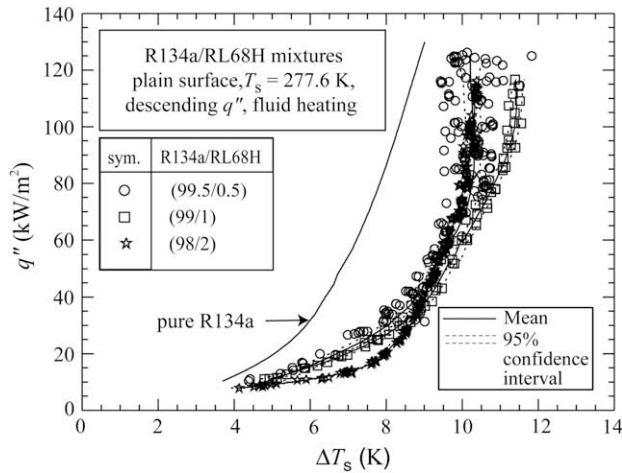


Fig. 4 – R134a/RL68H mixtures' boiling curves for plain surface.

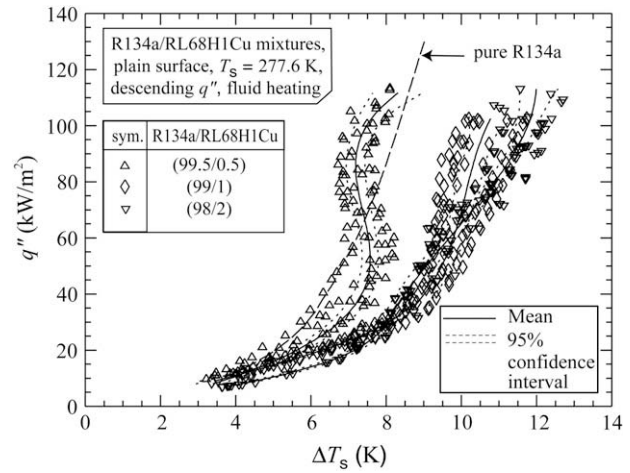


Fig. 5 – R134a/RL68H with 1% volume CuO mixtures' boiling curves for plain surface.

characteristic of having an enhanced boiling performance as compared to the R134a/RL68H1Cu (99/1) mixture. For most heat fluxes, the R134a/RL68H1Cu (99.5/0.5) superheat measurements, represented by the open triangles, are significantly less than those of the 99/1 and the 98/2 mixtures. For comparison, the mean of the pure R134a boiling curve is provided as a coarsely dashed line. The average expanded uncertainty of the estimated mean wall superheat for the three refrigerant/nanolubricant mixtures was 0.23 K.

A more precise comparison of the R134a/RL68H and the R134a/RL68H1Cu heat transfer performances relative to R134a and R134a/RL68H, respectively, is given in Figs. 6 and 7. Fig. 6 plots the ratio of the R134a/RL68H mixture heat flux to the pure R134a heat flux (q''_{PL}/q''_p) versus the pure R134a heat flux (q''_p) at the same wall superheat. Fig. 6 illustrates the influence of lubricant mass composition on the R134a/RL68H boiling curve with solid lines representing the mean heat flux ratios for each mixture. Overall, lubricant for all compositions has caused a heat transfer degradation relative to the heat transfer of pure R134a for all measured q''_p . The degradation is shown to increase with lubricant mass fraction. For example, the average heat flux ratio for the R134a/RL68H (99.5/0.5), the R134a/RL68H (99/1), and the R134a/RL68H (98/2) mixture from approximately 15 kW/m² to 120 kW/m² was 0.43, 0.37, and 0.28, respectively.⁴ The minimum heat transfer degradation for each mixture (or the maximum heat transfer) is shown in Fig. 6 to be at lowest measured heat fluxes. For 20 kW/m², the heat flux ratio for the R134a/RL68H (99.5/0.5), the R134a/RL68H (99/1), and the R134a/RL68H (98/2) mixture is 0.62 ± 0.16 , 0.58 ± 0.16 , and 0.47 ± 0.12 , respectively. The lubricant effect becomes more pronounced as the heat flux increases from roughly 20 kW/m² to 120 kW/m² producing heat flux ratios of approximately 0.37, 0.3, and 0.25 at 100 kW/m² for the R134a/

RL68H (99.5/0.5), the R134a/RL68H (99/1), and the R134a/RL68H (98/2) mixtures, respectively.

Fig. 7 details the effect that the CuO nanoparticles had on the R134a/RL68H boiling curves. The figure plots the ratio of the R134a/RL68H1Cu heat flux to the R134a/RL68H heat flux (q''_{CuO}/q''_{PL}) versus the R134a/RL68H1Cu mixture heat flux (q''_{CuO}) at the same wall superheat. The three different compositions are represented by three different lines where each R134a/nanolubricant mixture is compared to the R134a/pure-lubricant mixture at the same mass fraction. A heat transfer enhancement exists where the heat flux ratio is greater than one and the 95% simultaneous confidence intervals (depicted by the shaded regions) do not include the value one. Fig. 7 shows that the R134a/RL68H1Cu (99.5/0.5) mixture exhibits a significant boiling heat transfer enhancement over that of the R134a/RL68H (99.5/0.5) mixture. The heat flux ratio varies between roughly 1.5 and 3.75 for the R134a/RL68H1Cu (99.5/0.5) mixture for heat fluxes between 10 kW/m² and 110 kW/m². The R134a/RL68H1Cu (99/1) mixture shows a maximum heat flux ratio of approximately 1.54 and a region between 30 kW/m² and 60 kW/m² where no difference can be established between the two fluids because the confidence intervals include the value of one. Overall, the average heat flux ratio for the R134a/RL68H1Cu (99.5/0.5) mixture and the R134a/RL68H1Cu (99/1) mixture from approximately 10 kW/m² to 110 kW/m² was 2.4, and 1.19, respectively. The average heat flux ratio for the R134a/RL68H1Cu (98/2) mixture from approximately 10 kW/m² to 65 kW/m² was 1.12.

6. Discussion

The heat transfer results summarized in Fig. 7 show that nanolubricants have a great potential for improving the pool-boiling heat transfer of refrigerant/lubricant mixtures. However, Fig. 8 brings into question whether this enhancement is caused by an increase in thermal conductivity, as suggested in the Introduction, or some other mechanism(s).

⁴ A heat transfer enhancement for the R134a/RL68H (98/2) mixture is not shown because this occurs for values of q''_p larger than what was measured. Therefore, a comparison could not be made between the fluids at the larger heat flux.

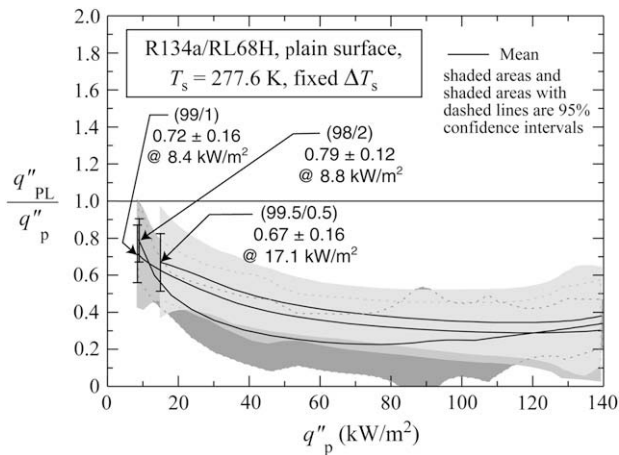


Fig. 6 – R134a/RL68H mixture heat flux relative to that of pure R134a for a plain surface.

Fig. 8 shows the thermal conductivity of several RL68H/CuO nanoparticle mixtures as measured with a transient line-source technique (Roder et al., 2000). Even though the thermal conductivity of CuO (20 W/m K, Kwak and Kim, 2005) is two orders of magnitude greater than that of neat RL68H (0.132 W/m K \pm 0.001 W/m K⁵), an improvement in the thermal conductivity significantly beyond that proportional to the volume fraction of the nanofluid was not obtained. For example, the volume fraction used in the boiling experiments (1%) resulted in the nanofluid having a thermal conductivity that is roughly 5% greater than that of the pure base fluid. This proportional improvement is disappointing compared to the 40% improvement in thermal conductivity for a 0.4% volume fraction achieved by Eastman et al. (2001). However, as shown in Fig. 8, the solid-liquid thermal conductivity model of Wasp (1977) confirms the measured thermal conductivity of the 1% by volume mixture (0.139 W/m K \pm 0.001 W/m K) to within approximately 4%.

The marginal increase in thermal conductivity of the refrigerant mixture as charged may not necessarily translate into marginal improvement of the thermal conductivity of the liquid at the heat transfer surface. The effective enhancement of the lubricant's thermal conductivity may in fact be greater than what the bulk concentration suggests because of the accumulation of nanoparticles in the lubricant excess layer that exists on the heat transfer surface. The increase in nanoparticle concentration in the excess layer was supported by observing the darkened lubricant that remained on the test surface after testing and removing the charge from the test apparatus. As a result, the thermal conductivity of the lubricant that resides on the surface and governs the boiling process may be greater than what the bulk nanoparticles concentration would suggest.

In order to more closely examine the effect of thermal conductivity, Fig. 9 compares the enhancement ratio for the

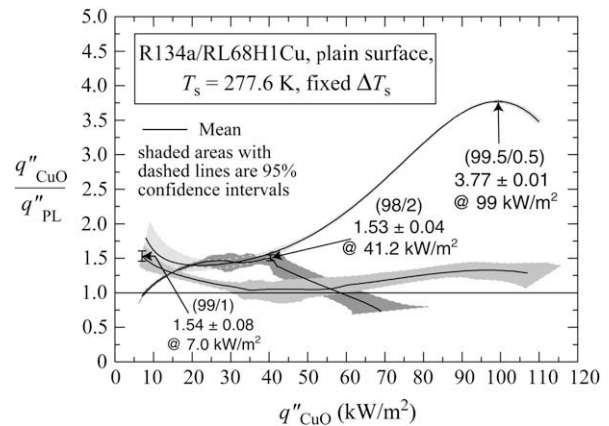


Fig. 7 – Boiling heat flux of R134a/RL68H1Cu mixtures relative to that of R134a/RL68H for a plain surface.

R134a/RL68H1Cu (99.5/0.5) mixture to those predicted by the refrigerant/lubricant mixture, pool-boiling model given in Kedzierski (2003b). The model is used to assess the effect of increased lubricant thermal conductivity on the boiling heat transfer. One prediction is presented for the charged 1% volume fraction corresponding to a nanolubricant thermal conductivity of 0.139 W/m K. The other prediction is presented to simulate the case where the nanoparticles accumulate to a 9% volume fraction on the heat transfer surface giving a thermal conductivity of 0.206 W/m K \pm 0.002 W/m K. Both predictions are at least 80% less than the measured heat flux ratio. Consequently, the comparison demonstrates that the increased thermal conductivity of the nanofluid cannot be used to explain the entire enhancement associated with the refrigerant/nanolubricant boiling heat transfer. It appears that at most, 20% of the enhancement may be due to increased thermal conductivity for a 9% volume fraction excess layer. Other factors are likely to contribute to the enhancement, for example, the particles may be inducing secondary nucleation on the bubbles and on the heat

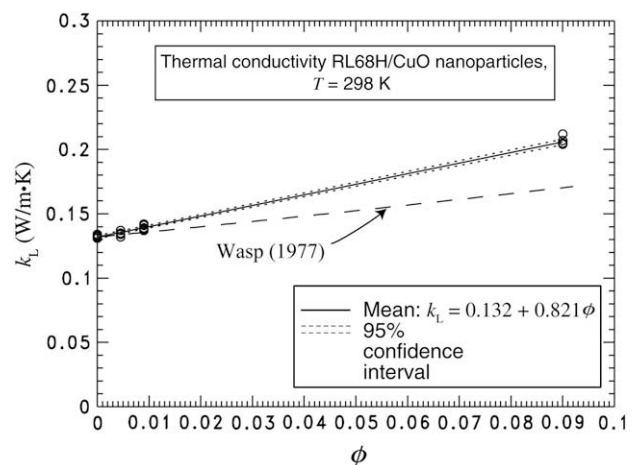


Fig. 8 – Measured thermal conductivity of RL68H/CuO nanoparticle mixtures as a function of volume fraction of CuO.

⁵ This is a random uncertainty obtained solely from repeated measurements, which does not account for a possible bias error. The type B uncertainty obtained from the manufacturer was \pm 0.01 W/m K.

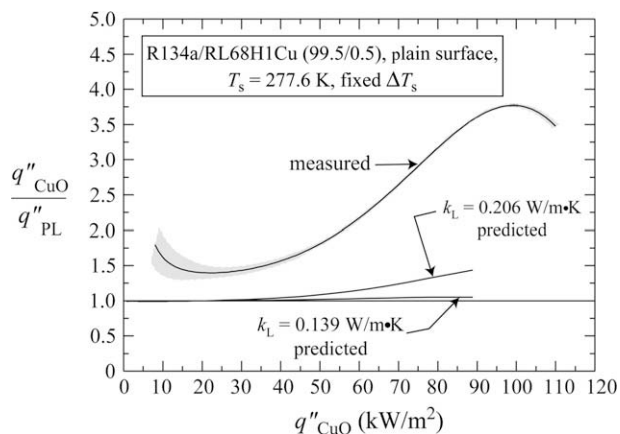


Fig. 9 – Predicted heat flux ratio for RL68H1Cu (99.5/0.5) mixture using Kedzierski (2003b) model.

transfer surface. The particles may be agglomerating within the excess layer and acting similar to a porous surface in enhancing boiling. In addition, there may be particle-mixing effects that contribute to the heat transfer enhancement. Conversely, heat transfer degradations may arise from nanoparticles filling the surface cavities (Jackson et al., 2006; Kedzierski, 2007).

Future research is required to investigate the influence of the particle material, its shape, size, distribution, and concentration on refrigerant boiling performance. Not only should the bulk concentration be studied, the distribution of the concentration of the nanoparticles within a particular system should be investigated. Because of the instability of the nanoparticles in the low viscosity refrigerant, the balance between the entrainment of nanoparticles by fluid mixing (rather than Brownian motion) and the deposition of nanoparticles in the excess layer will, in part, determine the distribution of nanoparticles in a particular system. In addition, a smaller fraction of the nanoparticles may be held up in monolayers to the wetted adiabatic surfaces. Hence, several interacting mechanisms are likely to be responsible for the distribution of nanoparticles in the system and, in turn, the performance of the system. For this reason, the influence of refrigerant/nanolubricant charge, heat transfer area, and adiabatic surface area on the concentration of the nanoparticles in the lubricant excess layer should be investigated. The potential for nanoparticles to travel to the heat transfer surface by the act of boiling is dictated by the available mass of nanoparticles in the refrigerant mixture charge. Consequently, it may not be fair to compare studies at the same bulk nanoparticles concentration for two different systems because the relative refrigerant-charge-to-surface area may differ for the two systems. Considering this, a parameter more pertinent than the bulk nanoparticles concentration for investigation may be the concentration of nanoparticles in the nanolubricant excess layer that resides on the boiling surface. Further investigation into the above effects may lead to a theory that can be used to develop nanolubricants that improve boiling heat transfer for the benefit of the refrigeration and air-conditioning industry.

7. Conclusions

The effect of CuO nanoparticles on the boiling performance of R134a/polyolester mixtures on a roughened, horizontal flat surface was investigated. A nanolubricant containing CuO nanoparticles at 1% volume fraction with a polyolester lubricant was mixed with R134a at three different mass fractions. For the 0.5% nanolubricant mass fraction, the nanoparticles caused a heat transfer enhancement relative to the heat transfer of pure R134a/polyolester (99.5/0.5) between 50% and 275%. A smaller enhancement was observed for the R134a/nanolubricant (99/1) mixture, which had a heat flux that was on average 19% larger than that of the R134a/polyolester (99/1) mixture. Further increase in the nanolubricant mass fraction to 2% resulted in a still smaller boiling heat transfer improvement of approximately 12% on average for the R134a/nanolubricant (98/2) mixture. The measurements illustrate that the performance improvement decreases with increasing lubricant concentration. Consequently, if a system can be designed to maintain a small lubricant concentration in the evaporator, significant performance improvements can be expected.

Although the nanoparticles increased the thermal conductivity of the lubricant, the increase in thermal conductivity appears to be responsible for only a small portion (potentially 20%) of the boiling heat transfer enhancement. Other effects, in particular, secondary nucleation and particle mixing may contribute more significantly to the enhancement of the refrigerant/lubricant boiling heat transfer with nanoparticles.

Acknowledgements

This work was funded by NIST. Thanks go to the following NIST personnel for their constructive criticism of the first draft of the manuscript: Mr. B. Dougherty, and Dr. P. Domaniski. Thanks go to Prof. A. Jacobi of the University of Illinois at Urbana-Champaign and to Prof. James Bryan of the University of Missouri-Columbia for their constructive criticisms of the second draft of the manuscript. Furthermore, the authors extend appreciation to W. Guthrie and Mr. A. Heckert of the NIST Statistical Engineering Division for their consultations on the uncertainty analysis. Some boiling heat transfer measurements were taken by Mr. David Wilmering of KT Consultants. The RL68H (EMKARATE RL 68H) was donated by Dr. S. Randles of Uniqema. The RL68H1Cu was manufactured by Nanophase Technologies with a copper (II) oxide and dispersant in RL68H especially for NIST.

REFERENCES

- Bang, I.C., Chang, S.H., 2004. Boiling heat transfer performance and phenomena of Al_2O_3 -water nanofluids from a plain surface in a pool. In: Proceedings of ICAPP. Pittsburgh, PA. pp. 1437-1443.
- Belsley, D.A., Kuh, E., Welsch, R.E., 1980. Regression Diagnostics: Identifying Influential Data and Sources of Collinearity. Wiley, New York.
- Bi, S., Shi, L., Zhang, L., 2007. Performance study of a domestic refrigerator using R134a/mineral oil/nano-TiO₂ as working

- fluid. In: Proceedings of Int. Congress of Refrigeration, ICR07-B2-346. Beijing, China.
- Eastman, J.A., Choi, S.U.S., Li, S., Yu, W., Thompson, L.J., 2001. Anomalous increased effective thermal conductivities of ethylene glycol-based nanofluids containing copper nanoparticles. *Appl. Phys. Lett.* 78, 718-720.
- Jackson, J.E., Borgmeyer, B.V., Wilson, C.A., Cheng, P., Bryan, J.E., 2006. Characteristics of nucleate boiling with gold nanoparticles in water. In: Proceedings of IMECE2006. Chicago, IL. IMECE2006-16020.
- Kedzierski, M.A., Gong, M., 2007. Effect of CuO Nanolubricant on R134a Pool Boiling Heat Transfer with Extensive Measurement and Analysis Details. NISTIR 7454. U.S. Department of Commerce, Washington, DC.
- Kedzierski, M.A., 2007. Effect of CuO nanoparticle concentration on R134a/lubricant pool boiling heat transfer. In: Proceedings of the ASME Micro/Nanoscale Heat Transfer International Conference. Tainan, Taiwan. IMECE MNHT2008-52116.
- Kedzierski, M.A., 2006. A comparison of R245fa pool boiling measurements to R123, and R245fa/isopentane on a passively enhanced, horizontal surface. *Int. J. Transport Phenom.* 8 (4), 331-344.
- Kedzierski, M.A., 2003a. A semi-theoretical model for predicting R123/lubricant mixture pool boiling heat transfer. *Int. J. Refrigeration* 26, 337-348.
- Kedzierski, M.A., 2003b. Improved thermal boundary layer parameter for semi-theoretical refrigerant/lubricant pool boiling model. In: Proceedings of Int. Congress of Refrigeration, ICR0504. Washington, DC.
- Kedzierski, M.A., 2002. Use of fluorescence to measure the lubricant excess surface density during pool boiling. *Int. J. Refrigeration* 25, 1110-1122.
- Kedzierski, M.A., 2001a. Use of Fluorescence to Measure the Lubricant Excess Surface Density During Pool Boiling. NISTIR 6727. U.S. Department of Commerce, Washington, DC.
- Kedzierski, M.A., 2001b. The effect of lubricant concentration, miscibility and viscosity on R134a pool boiling. *Int. J. Refrigeration* 24 (4), 348-366.
- Kedzierski, M.A., 2000. Enhancement of R123 pool boiling by the addition of hydrocarbons. *Int. J. Refrigeration* 23, 89-100.
- Kedzierski, M.A., 1995. Calorimetric and Visual Measurements of R123 Pool Boiling on Four Enhanced Surfaces. NISTIR 5732. U.S. Department of Commerce, Washington.
- Kwak, K., Kim, C., 2005. Viscosity and thermal conductivity of copper oxide nanofluid dispersed in ethylene glycol. *Korea-Aust Rheol J.* 17 (2), 35-40.
- Memory, S.B., Marto, P.J., 1992. The influence of oil on boiling hysteresis of R-114 from enhanced surfaces. In: Proceedings of the ASME Engineering Foundation Conference on Pool and External Flow Boiling, Santa Barbara, CA, pp. 63-71.
- Roder, H.M., Perkins, R.A., Laesecke, A., Nieto de Castro, C.A., 2000. Absolute steady-state thermal conductivity measurements by use of a transient hot-wire system. *J. Res. Natl. Inst. Stand. Technol.* 105 (2), 221-253.
- Sung, L., 2006. Private Communications, National Institute of Standards and Technology. Building and Fire Research Laboratory, Gaithersburg, MD.
- Wasp, F.J., 1977. Solid-Liquid Flow Slurry Pipeline Transportation. *Trans., Tech. Pub., Berlin.*
- Wen, D., Ding, Y., 2005. Experimental investigation into the pool boiling heat transfer of aqueous based γ -alumina nanofluids. *J. Nanopart Res.* 7, 265-274.
- You, S.M., Kim, J.H., Kim, K.H., 2003. Effect of nanoparticles on critical heat flux of water in pool boiling heat transfer. *Appl. Phys. Lett.* 83 (16), 375-377.